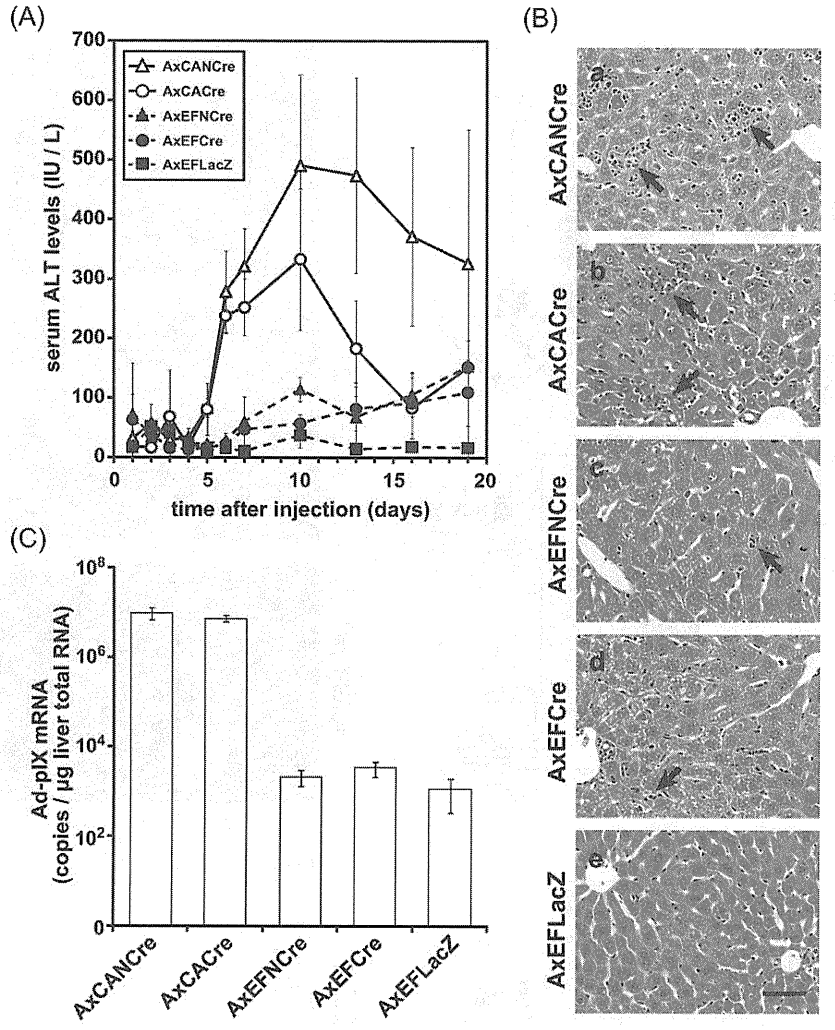

Fig. 3. Effects of AdVs on liver injuries in HCV transgenic mice. (A) Serum ALT levels were measured at the indicated time-points in CN2-29 transgenic mice injected with 1.0×10^9 PFU AxCANCre (open triangle), AxCACre (open circle), AxEFNCre (closed triangle), AxEFCre (closed circle), and AxEFLacZ (closed rectangle). The ALT levels are shown as means ± S.D. of three individual specimens. (B) Histopathologic changes in the livers of transgenic mice 7 days after injection of each AdV. The liver sections were stained with H&E. The arrows represent lymphocyte infiltrations. Scale bar, 50 μm. (C) mRNA expression of Ad-pIX in the livers. CN2-29 transgenic mice were injected with 1.0×10^9 PFU of the AdVs. After 12 h, the livers were harvested. The total RNA extracts from the livers were subjected to reverse transcription and RTD-PCR with an Ad-pIX-specific probe and a primer pair, as described in Section 2. The numbers of copies of Ad-pIX mRNA are shown as means ± S.D. of three individual specimens.

reverse transcription and quantitative RTD-PCR, as described under Section 2. The copy numbers of Ad-pIX mRNA were quite high in transgenic mice that were injected with AdV bearing the CAG promoter (Fig. 3C). The observed inflammation levels were consistent with the expression levels of Ad-pIX.

3.4. *Liver inflammatory responses to the HCV protein inducibly expressed by AdVs in transgenic mice*

Because our results indicated that severe liver injuries were caused by AdVs bearing the CAG promoter, we evaluated liver inflammatory responses to the HCV protein inducibly expressed by AdVs in transgenic mice 7 days post-injection according to the modified HAI scoring system (Fig. 4A) (Knodell et al., 1981; Yang et al., 1994). Among the transgenic mice, more severe liver damage was observed in those that were injected with Cre-expressing AdVs bearing the CAG promoter (Fig. 4A, AxCANCre and AxCACre) compared to those injected with Cre-expressing AdVs bearing the EF1α promoter (Fig. 4A, AxEFNCre and AxEFCre).

Because AxEFCre more efficiently expressed HCV proteins than AxEFNCre (Fig. 2C and D), we injected AxEFCre into transgenic mice and wild-type mice to examine the effects of HCV protein expression. The severity of liver inflammation in the AxEFCre-injected transgenic mice was significantly greater than in the AxEFCre-injected wild-type mice or the AxEFLacZ-injected transgenic mice (Fig. 4A and B).

Seven days after AdV administration, serum ALT levels of AxCANCre-injected wild-type mice were significantly higher than those of AxEFCre-injected wild-type mice (Fig. 4C). This ALT elevation was observed in both transgenic and wild-type mice injected with AxCANCre (Fig. 4C). In contrast, AxEFCre was injected into the two groups, transgenic mice expressing HCV proteins exhibited more severe liver injury than wild-type mice (Fig. 4C and D).

3.5. *Effects of Cre-expressing AdV bearing the EF1α promoter on HCV protein expression in transgenic mouse livers*

To investigate whether CN2-29 transgenic mice injected with AdVs bearing the EF1α promoter showed liver inflammation caused

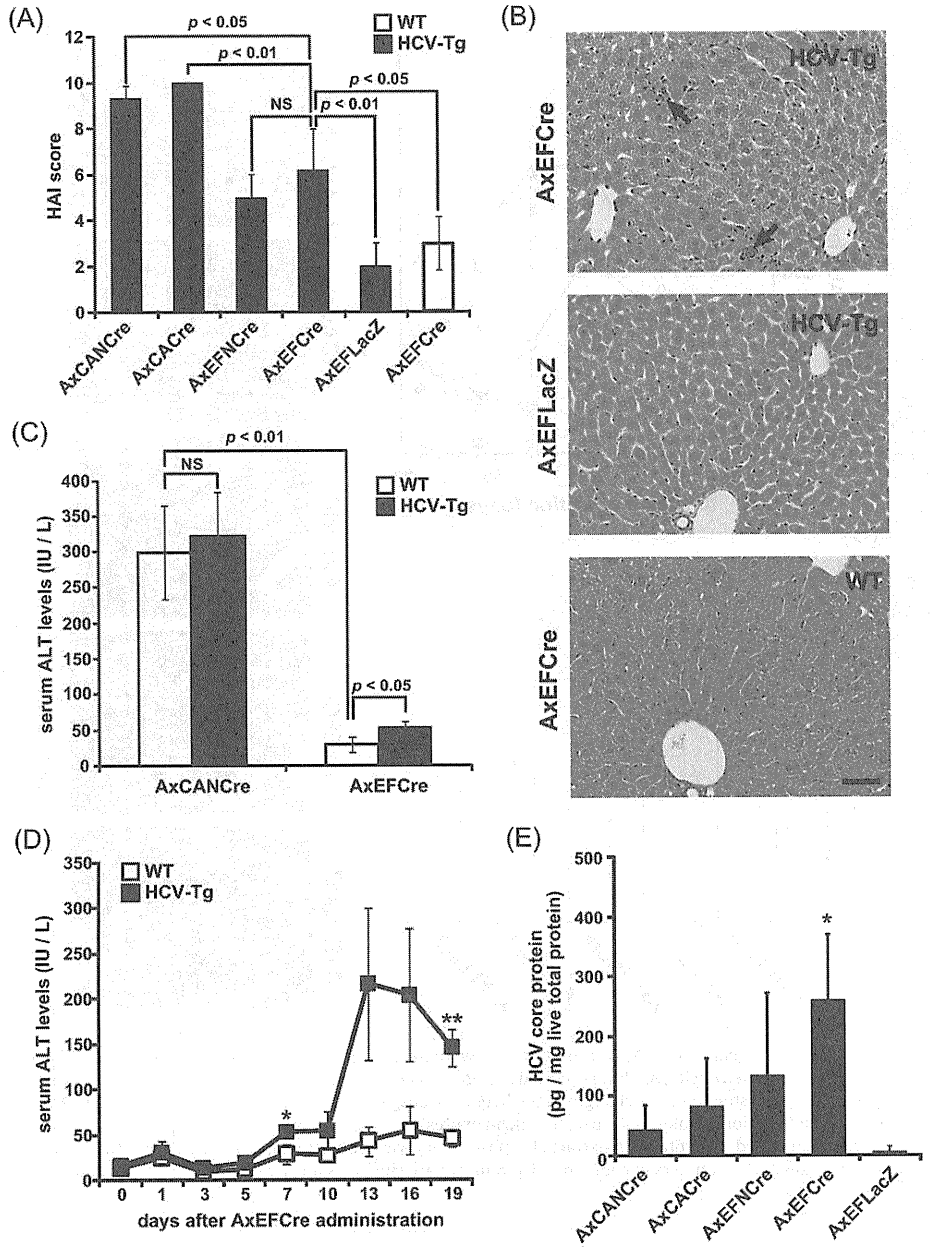

Fig. 4. Liver inflammatory responses due to HCV protein expression induced by AxEFCre. (A) Histopathology of mouse livers after injection of AdVs. Histopathologic features of the livers of CN2-29 transgenic mice (HCV-Tg, closed bars) injected with 1.0×10^9 PFU of AxCANCre, AxCACre, AxEFNCre, AxEFCre, or AxEFLacZ, and wild-type mice that were injected with 1.0×10^9 PFU of AxEFCre at day 7 post-injection (WT, opened bar). Pathologic changes were evaluated by light microscopy of H&E-stained sections of the mouse livers using the modified HAI scoring system. The extent of pathology was scored on a scale from 0 (none) to 12 (severe). All of the scores are means ± S.D. of more than three individual specimens. Statistical analysis was performed using an unpaired Student's *t*-test. NS, not significant. (B) Histopathologic changes resulting from HCV protein expression in mouse livers. CN2-29 transgenic mice (HCV-Tg) were injected with AxEFCre or AxEFLacZ and wild-type mice (WT) were injected with AxEFCre 7 days post-injection. The liver sections were stained with H&E. The arrows represent piecemeal necrosis. Scale bars, 50 μm. (C) Serum ALT levels with or without HCV protein expression 7 days after administration of the AdVs. Statistical analysis was performed using an unpaired Student's *t*-test between CN2-29 transgenic mice (HCV-Tg) and wild-type mice (WT). NS, not significant. (D) Sequential changes in serum ALT levels after AxEFCre administration. Serum ALT levels were measured at the indicated time-points in CN2-29 transgenic mice (HCV-Tg, closed square) or wild-type mice (WT, opened square) that were injected with 1.0×10^9 PFU AxEFCre. ALT levels are shown as means ± S.D. of more than three individual specimens. Statistical analysis was performed using an unpaired Student's *t*-test between CN2-29 transgenic mice (HCV-Tg) and wild-type mice (WT). $^*p < 0.05$; $^{**}p < 0.01$. (E) HCV core protein expression 21 days after AdV administration in transgenic mouse livers. CN2-29 transgenic mice were injected with 1.0×10^9 PFU for each AdV. After 21 days, the livers were harvested and homogenized. The concentrations of HCV core proteins in liver lysates were determined by EIA. The values shown are means ± S.D. of three individual experiments. Statistical analysis was performed using an ANOVA, followed by the SNK test. $^*p < 0.05$.

by persistently expressed HCV proteins, we evaluated core proteins by EIA in transgenic mouse livers 21 days post-injection of the AdVs (Fig. 4E). HCV core protein expression was scarcely detectable in the transgenic mice injected with AxCANCre, while the AxEFCre-injected transgenic mice showed significantly higher levels of core protein expression (Fig. 4E). Although, the AxCANCre injection was scarcely observed at day 21 in the transgenic mice (Fig. 4E), HCV core protein expression induced by AxEFCre injection was observed until at least day 56.

4. Discussion

In the present study, we demonstrated that Cre-expressing AdVs bearing the EF1α promoter induce HCV gene expression and

HCV protein production without induction of severe liver injury in inducible-HCV transgenic mice. We further observed that increases in serum ALT levels and liver inflammation were related to HCV protein expression mediated by AxEFCre injection. Moreover, AxEFCre injection enabled the transgenic mice to persistently express HCV proteins.

In previous studies, HCV transgenic mice constitutively expressing HCV proteins exhibited symptoms of steatosis and/or hepatocellular carcinoma, but did not show inflammatory or immunopathologic changes (Lerat et al., 2002; Moriya et al., 1997, 1998; Sun et al., 2001). Inducible-HCV transgenic mouse lineages, in which HCV protein expression is regulated, have enabled investigation of the immunopathogenesis of HCV protein expression. HCV transgenic mice regulated by the Cre/*lox*P system (Sun et al., 2005; Tumurbaatar et al., 2007; Wakita et al., 1998) or the tetracycline regulatory system (Ernst et al., 2007) exhibit inducible and liver-specific expression of HCV proteins. Inducible-HCV transgenic mice using the Cre/*lox*P system with an AdV that expresses Cre under the control of the CAG promoter (AxCANCre) exhibit HCV-specific immune responses (Wakita et al., 1998, 2000). The inducible-HCV CN2-29 transgenic mice, which express the core, E1, E2, and NS2 proteins, have HCV-specific cytotoxic T lymphocytes (Takaku et al., 2003; Wakita et al., 1998, 2000).

However, they show severe inflammatory responses to AxCANCre itself and thus, HCV protein expression is only transient (Wakita et al., 2000). These significant obstacles have limited the utility of inducible-HCV transgenic mice. Therefore, to deliver the *Cre* gene into the liver, non-adenoviral induction methods have been developed (Ho et al., 2008; Sun et al., 2005; Zhu et al., 2006). Meanwhile, adenoviral genes that cause cellular immune responses have been identified and modified AdVs that do not trigger host immune responses have been developed (Palmer and Ng, 2005). A recent study demonstrated that immune responses to AdVs bearing the CAG promoter were associated with co-expression of Ad-pIX, whereas immune responses were minimal when transgene expression was controlled by the EF1α promoter (Nakai et al., 2007). Therefore, we postulated that severe inflammation of mouse livers after administration of Cre-expressing AdVs bearing the CAG promoter (AxCANCre) might be caused by expression of Ad-pIX. In the present study, we generated Cre-expressing AdVs bearing the EF1α promoter (AxEFCre) and infected HCV transgenic mice. AxEFCre-injected mice expressed much less Ad-pIX mRNA and did not show the increased levels of ALT or severe liver inflammation as did Cre-expressing AdVs under the control of the CAG promoter (Fig. 3). In contrast, AxCANCre administration caused severe liver injury in both HCV transgenic mice and wild-type mice (Fig. 4D; Wakita et al., 2000). AxEFCre administration caused liver injury in the HCV transgenic mice, but not in the wild-type mice (Fig. 4A–D). These results suggest that AxEFCre alone induces only minimal host immune responses compared to AxCANCre; therefore, the liver inflammatory responses exhibited by AxEFCre-injected transgenic mice were clearly due to expression of HCV proteins. Because AxCANCre injection alone causes severe liver injuries, most of the hepatocytes infected with AxCANCre are eliminated and HCV protein expression in the livers of transgenic mice is only transient (Wakita et al., 2000). On the other hand, AxEFCre injection did not induce such severe liver injuries. The AxEFCre-injected HCV transgenic mice showed milder liver inflammation in response to expression of HCV proteins and persistently expressed HCV proteins without elimination of hepatocytes infected with AxEFCre.

In conclusion, HCV gene expression mediated by the Cre/*lox*P system and a Cre-expressing AdV that bears the EF1α promoter, AxEFCre, enables Cre-mediated recombination of transgenes in mice without inducing severe liver injury due to the AdV itself. Moreover, this inducible-HCV transgenic mouse model should be useful for investigation of liver injury due to HCV and the pathogenesis of HCV.

Acknowledgments

The authors wish to thank Mitsugu Takahashi for breeding the transgenic mice. This study was supported by grants from the Ministry of Education, Culture, Sports, Science and Technology of Japan; the Program for Promotion of Fundamental Studies in Health Sciences of the Pharmaceuticals and Medical Devices Agency of Japan; and the Ministry of Health, Labor and Welfare of Japan.

References

Akagi, K., Sandig, V., Vooijs, M., Van der Valk, M., Giovannini, M., Strauss, M., Berns, A., 1997. Cre-mediated somatic site-specific recombination in mice. Nucleic Acids Res. 25 (9), 1766–1773.

Baba, Y., Nakano, M., Yamada, Y., Saito, I., Kanegae, Y., 2005. Practical range of effective dose for Cre recombinase-expressing recombinant adenovirus without cell toxicity in mammalian cells. Microbiol. Immunol. 49 (6), 559–570.

Bangari, D.S., Mittal, S.K., 2006. Current strategies and future directions for eluding adenoviral vector immunity. Curr. Gene Ther. 6 (2), 215–226.

Ernst, E., Schonig, K., Bugert, J.J., Blaker, H., Pfaff, E., Stremmel, W., Encke, J., 2007. Generation of inducible hepatitis C virus transgenic mouse lines. J. Med. Virol. 79 (8), 1103–1112.

Goodman, Z.D., Ishak, K.G., 1995. Histopathology of hepatitis C virus infection. Semin. Liver Dis. 15 (1), 70–81.

Ho, K.J., Bass, C.E., Kroemer, A.H., Ma, C., Terwilliger, E., Karp, S.J., 2008. Optimized adeno-associated virus 8 produces hepatocyte-specific Cre-mediated recombination without toxicity or affecting liver regeneration. Am. J. Physiol. Gastrointest. Liver Physiol. 295 (2), G412–G419.

Kafri, T., Morgan, D., Krahl, T., Sarvetnick, N., Sherman, L., Verma, I., 1998. Cellular immune response to adenoviral vector infected cells does not require de novo viral gene expression: implications for gene therapy. Proc. Natl. Acad. Sci. U S A 95 (19), 11377–11382.

Kanegae, Y., Lee, G., Sato, Y., Tanaka, M., Nakai, M., Sakaki, T., Sugano, S., Saito, I., 1995. Efficient gene activation in mammalian cells by using recombinant adenovirus expressing site-specific Cre recombinase. Nucleic Acids Res. 23 (19), 3816–3821.

Kanegae, Y., Makimura, M., Saito, I., 1994. A simple and efficient method for purification of infectious recombinant adenovirus. Jpn. J. Med. Sci. Biol. 47 (3), 157–166.

Knodell, R.G., Ishak, K.G., Black, W.C., Chen, T.S., Craig, R., Kaplowitz, N., Kiernan, T.W., Wollman, J., 1981. Formulation and application of a numerical scoring system for assessing histological activity in asymptomatic chronic active hepatitis. Hepatology 1 (5), 431–435.

Kobayashi, N., Fujiwara, T., Westerman, K.A., Inoue, Y., Sakaguchi, M., Noguchi, H., Miyazaki, M., Cai, J., Tanaka, N., Fox, I.J., Leboulch, P., 2000. Prevention of acute liver failure in rats with reversibly immortalized human hepatocytes. Science 287 (5456), 1258–1262.

Kremsdorf, D., Brezillon, N., 2007. New animal models for hepatitis C viral infection and pathogenesis studies. World J. Gastroenterol. 13 (17), 2427–2435.

Lerat, H., Honda, M., Beard, M.R., Loesch, K., Sun, J., Yang, Y., Okuda, M., Gosert, R., Xiao, S.Y., Weinman, S.A., Lemon, S.M., 2002. Steatosis and liver cancer in transgenic mice expressing the structural and nonstructural proteins of hepatitis C virus. Gastroenterology 122 (2), 352–365.

Moriya, K., Fujie, H., Shintani, Y., Yotsuyanagi, H., Tsutsumi, T., Ishibashi, K., Matsuura, Y., Kimura, S., Miyamura, T., Koike, K., 1998. The core protein of hepatitis C virus induces hepatocellular carcinoma in transgenic mice. Nat. Med. 4 (9), 1065–1067.

Moriya, K., Yotsuyanagi, H., Shintani, Y., Fujie, H., Ishibashi, K., Matsuura, Y., Miyamura, T., Koike, K., 1997. Hepatitis C virus core protein induces hepatic steatosis in transgenic mice. J. Gen. Virol. 78 (7), 1527–1531.

Nakai, M., Komiya, K., Murata, M., Kimura, T., Kanaoka, M., Kanegae, Y., Saito, I., 2007. Expression of pIX gene induced by transgene promoter: possible cause of host immune response in first-generation adenoviral vectors. Hum. Gene. Ther. 18 (10), 925–936.

Palmer, D.J., Ng, P., 2005. Helper-dependent adenoviral vectors for gene therapy. Hum. Gene. Ther. 16 (1), 1–16.

Shepard, C.W., Finelli, L., Alter, M.J., 2005. Global epidemiology of hepatitis C virus infection. Lancet Infect. Dis. 5 (9), 558–567.

Shintani, Y., Yotsuyanagi, H., Moriya, K., Fujie, H., Tsutsumi, T., Kanegae, Y., Kimura, S., Saito, I., Koike, K., 1999. Induction of apoptosis after switch-on of the hepatitis B virus X gene mediated by the Cre/loxP recombination system. J. Gen. Virol. 80 (12), 3257–3265.

Sun, J., Bodola, F., Fan, X., Irshad, H., Soong, L., Lemon, S.M., Chan, T.S., 2001. Hepatitis C virus core and envelope proteins do not suppress the host's ability to clear a hepatic viral infection. J. Virol. 75 (24), 11992–11998.

Sun, J., Tumurbaatar, B., Jia, J., Diao, H., Bodola, F., Lemon, S.M., Tang, W., Bowen, D.G., McCaughan, G.W., Bertolino, P., Chan, T.S., 2005. Parenchymal expression of CD86/B7.2 contributes to hepatitis C virus-related liver injury. J. Virol. 79 (16), 10730–10739.

Takaku, S., Nakagawa, Y., Shimizu, M., Norose, Y., Maruyama, I., Wakita, T., Takano, T., Kohara, M., Takahashi, H., 2003. Induction of hepatic injury by hepatitis C-virus-

specific CD8± murine cytotoxic T lymphocytes in transgenic mice expressing the viral structural genes. Biochem. Biophys. Res. Commun. 301, 330–337.
Takeuchi, T., Katsume, A., Tanaka, T., Abe, A., Inoue, K., Tsukiyama-Kohara, K., Kawaguchi, R., Tanaka, S., Kohara, M., 1999. Real-time detection system for quantification of hepatitis C virus genome. Gastroenterology 116 (3), 636–642.
Tumurbaatar, B., Sun, Y., Chan, T., Sun, J., 2007. Cre-estrogen receptor-mediated hepatitis C virus structural protein expression in mice. J. Virol. Methods 146 (1–2), 5–13.
Wakita, T., Katsume, A., Kato, J., Taya, C., Yonekawa, H., Kanegae, Y., Saito, I., Hayashi, Y., Koike, M., Miyamoto, M., Hiasa, Y., Kohara, M., 2000. Possible role of cytotoxic T cells in acute liver injury in hepatitis C virus cDNA transgenic mice mediated by Cre/loxP system. J. Med. Virol. 62 (3), 308–317.
Wakita, T., Taya, C., Katsume, A., Kato, J., Yonekawa, H., Kanegae, Y., Saito, I., Hayashi, Y., Koike, M., Kohara, M., 1998. Efficient conditional transgene expression in hepatitis C virus cDNA transgenic mice mediated by the Cre/loxP system. J. Biol. Chem. 273 (15), 9001–9006.
Yang, Y., Ertl, H.C., Wilson, J.M., 1994. MHC class I-restricted cytotoxic T lymphocytes to viral antigens destroy hepatocytes in mice infected with E1-deleted recombinant adenoviruses. Immunity 1 (5), 433–442.
Zhu, H.Z., Wang, W., Feng, D.M., Sai, Y., Xue, J.L., 2006. Conditional gene modification in mouse liver using hydrodynamic delivery of plasmid DNA encoding Cre recombinase. FEBS Lett. 580 (18), 4346–4352.

Genes to Cells

Comparison of efficiency between FLPe and Cre for recombinase-mediated cassette exchange *in vitro* and in adenovirus vector production

Yuki Takata[a†], Saki Kondo[b†], Naoki Goda, Yumi Kanegae and Izumu Saito*

Laboratory of Molecular Genetics, Institute of Medical Science, University of Tokyo, 4-6-1 Shirokanedai, Minato-ku, Tokyo 108-8639, Japan

Cre and FLP recombinases mediate not only specific deletions and insertions, but also the recombinase-mediated cassette exchange (RMCE) reaction, which is used in cell biotechnology including ES cells and mouse genetics. However, comparison of efficiencies for Cre and FLP in RMCE has not been made. We here examined the detailed process of RMCE with Cre and FLP *in vitro* using mutant *lox*P 2272 and three mutant FRTs (FRT G, FRT H, and FRT F3) and then quantitatively compared the RMCE reactions *in vitro*. Interestingly, in the *in vitro* reactions, the RMCE efficiency of Cre reached a plateau level of approximately 5% and did not proceed further, whereas that of FLPe reached approximately 12–13%, showing that FLPe reached a higher level of efficiency than Cre possibly when they were supplied at a very high concentration. Moreover, we quantitatively compared the production efficiency of E1-deleted adenovirus vector using the RMCE method with Cre or FLP. The results showed that FLPe was again found more efficient than Cre in RMCE reaction. Thus, although Cre is considered more active than, or similar to, FLPe, it may not be necessarily true for RMCE reaction. Possible reasons explaining these results are discussed.

Introduction

Site-specific recombinases for the analysis of gene function are an important tool for both cultured cells and *in vivo* studies (for a review, see Akopian & Marshall Stark 2005; Grindley *et al.* 2006; Bischof & Basler 2008; Bucholtz 2008; Birling *et al.* 2009). Recombinases can induce the deletion, insertion, or inversion of DNA sequences by connecting two sequences without requiring any other factor; these DNA rearrangements can mediate gene activation and inactivation. FLP derived from *Saccharomyces cerevisiae* and Cre derived from bacteriophage P1 are well-characterized recombinases. They recognize a target sequence of 34-base pair (bp), and recombination occurs between two targets. Whereas Cre activity is stable at 37 °C, the optimum temperature of wild-type FLP (wtFLP) is approximately 30 °C because of its poor thermostability. This drawback has been largely overcome by the development of a thermostable mutant of FLP (FLPe) containing four amino acid substitutions (Buchholz *et al.* 1998). FLPe has been reported to work as effectively as Cre in somatic cell lines and mice (Farley *et al.* 2000; Rodriguez *et al.* 2000; Beard *et al.* 2006), but one report has shown that FLPe activity on chromosomal targets was only 10% of that of Cre (Andreas *et al.* 2002), and that in embryonic stem cells FLPe was less efficient than Cre (Schaft *et al.* 2001). Thus, FLPe activity is considered to be similar to or lower than that of Cre. Cre has been reported to be toxic to cells (Loonstra *et al.* 2001; Pfeifer *et al.* 2001; Baba *et al.* 2005), whereas FLP has never been reported to be toxic.

Communicated by: Tadashi Yamamoto
**Correspondence:* isaito@ims.u-tokyo.ac.jp
†These authors equally contributed in this work.
[a]*Present address*: Manufacturing Technology Koukandou Co., Ltd, 2-9-1, Umezawa-cho, Toyama-shi, Toyama 930-0055, Japan.
[b]*Present address*: Cell Regulation Laboratory, Paterson Institute for Cancer Research, University of Manchester, Wilmslow Road, Manchester M20 4BX, UK.

DOI: 10.1111/j.1365-2443.2011.01526.x

Recombinases can mediate another recombination activity: recombinase-mediated cassette exchange (RMCE) (for a review, see Oumard *et al.* 2006; Wirth *et al.* 2007), in which two DNA regions on different molecules are flanked by a wild-type (wt) and a mutant target sequence. Recombinase exchanges the two DNA regions flanked by the wt and mutant targets while maintaining the orientation of the regions. The RMCE method has been used in cells including ES cells and in mouse biotechnology. For an ideal RMCE reaction, the mutant target would not recombine with the wt target, but only with the identical mutant target. Such 'exclusive' mutant targets have been reported for FLPs, such as FRT F3 and FRT F5 (Schlake & Bode 1994), as well as for Cre, such as *lox*P 2272 (Lee & Saito 1998), which contains two transversion mutations and is identical to *lox*P V (Kondo *et al.* 2003; Nakano *et al.* 2005). In addition, FRT f2161 (denoted as FRT G in this paper) and FRT f2262 (denoted as FRT H) are newly identified and described 'exclusive' mutant FRTs possessing two nucleotide substitutions in the central spacer region (Nakano *et al.* 2001b). Although FLPe and Cre were used in RMCE, direct comparison of their efficiency has not yet been reported and the detailed *in vitro* process of RMCE has not been quantitatively studied. Other than FLP- and Cre-mediated RMCE, resolvase ΦC31 can also mediate the RMCE reaction (Belteki *et al.* 2003), although it has been reported to show a high background (Thyagarajan *et al.* 2001) and cell toxicity similar to Cre (Andreas *et al.* 2002).

We have established a quantitative *in vitro* assay system using lysates containing a high concentration of recombinase produced using adenovirus vector (AdV) in infected 293 cells, and the assay has successfully been used (Lee & Saito 1998; Nakano *et al.* 2001a,b; Kondo *et al.* 2009). The AdV-production system is very efficient, and the lysate contains a very high level of the recombinase because it was produced under the control of a very potent CAG promoter (Niwa *et al.* 1991), and the AdV vector replicates 100 000 copies per 293 cell. Another reason for using lysates is that they seem partly to reflect circumstances within mammalian cells.

Recently, we developed a method for the production of E1-deleted AdV using Cre-mediated RMCE (Nakano *et al.* 2005). The AdV possesses a very large genome of more than 30 kilobases (kb), and hence, all other production methods currently available must handle a very large plasmid or cosmid containing most of the AdV genome. In this method, an expression unit in a small donor plasmid is transferred onto a recipient AdV genome in Cre-expressing 293 cells using RMCE, and the desired AdV containing the DNA region selectively proliferates, because the AdV specifically acquires the lost packaging sequence (see Fig. 4A). However, the Cre-expressing 293 cells are very difficult to handle probably because of Cre toxicity, and the RMCE efficiency using FLPe has not yet been examined.

Here, we compared the RMCE efficiencies between FLPs and Cre in a quantitative *in vitro* assay and in AdV production. Interestingly, in the *in vitro* assay, the RMCE efficiency of FLPe was much higher than that of Cre, because that of Cre reached a plateau level and did not proceed further. Moreover, for AdV production, FLPe was again found more efficient than Cre. Thus, using RMCE, FLPe was more efficient than Cre in these cases.

Results

In vitro recombination of mutant FRTs using wtFLP and FLPe

In this study, three mutant FRTs were examined (Fig. 1): FRT G, FRT H (Nakano *et al.* 2001b), and FRT F3 (Schlake & Bode 1994) contain double and quadruple mutations and have been reported to show a high recombination efficiency with strict fidelity.

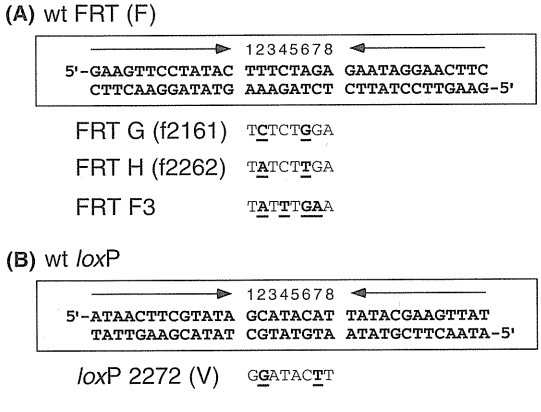

Figure 1 Nucleotide sequences of the recombinase targets used in this study. Arrows show the 13-nucleotide inverted repeats. Underlines show nucleotide differences from wt target sequence. (A) Sequences of wt FRT and mutant FRTs. The mutant FRTs, f2161 and f2262 (Nakano *et al.* 2001b), are named as FRT G and FRT H, respectively. The mutant FRT F3 has been previously reported (Schlake & Bode 1994). (B) Sequences of wt *lox*P and mutant *lox*P 2272 (Lee & Saito 1998; Kondo *et al.* 2003; Nakano *et al.* 2005). The *lox*P 2272 is called as V in the names of plasmids and adenovirus vectors.

To examine the efficiency of mutant-vs.-mutant recombination for each mutant FRT and wt FRT (denoted F), four plasmid substrates were newly constructed, each of which contained two identical wt or mutant FRTs (F and muF, Fig. 2A). A quantitative *in vitro* assay was carried out as described (Lee & Saito 1998; Nakano *et al.* 2001a,b) using lysate containing wt FLP enzyme expressed by AdV in 293 cells. The cell lysate was mixed with *Hin*dIII-linearized pCAFNFG substrate and reacted for 30 min at 30 °C for recombination; then, the DNA was extracted and digested with *Fsp*I (Fig. 2B); the substrate (S) produced bands of 2.3 and 2.8 kb, whereas 1.2- and 3.9-kb bands were yielded as Products (P) after recombination. The recombination efficiency after the addition of serial amounts of the wt FLP lysate was quantified by comparing the intensity of the bands of the copy-marker DNAs (an example is shown in Fig. 2C).

To evaluate the efficiency of mutant-vs.-mutant recombination, the results when using wtFLP lysate at 30 °C were shown in Fig. 2D, left panel. The order of efficiencies of the three mutant FRTs was FRT G > FRT F3 > FRT H, agreeing with the results of Nakano *et al.* (2001a). However, when FLPe lysate prepared using the FLPe-expressing AdV, AxCAFLPe, was used at 37 °C with the same substrates (Fig. 2D, right panel), the recombination efficiencies of the three mutant FRTs were FRT F3 > FRT H > FRT G, i.e. the order differed from that of wt FLP at 30 °C, with FRT G having the lowest efficiency. These results showed that the mutated FRT with the highest recombination efficiency when using wtFLP was not necessarily the highest mutated FRT when using FLPe.

To examine the efficiency of wt FRT-vs.-mutant recombination of FRT G, FRT H or FRT F3, plasmids of pCAFNGG, pCAFNHG, and pCAFNF3G were constructed and assayed for wt FLP and FLPe. No recombination product was detected, showing that all of these mutant FRTs were 'exclusive' both in wt FLP (Nakano *et al.* 2001a) and in FLPe (data not shown), within the limit of the detection level.

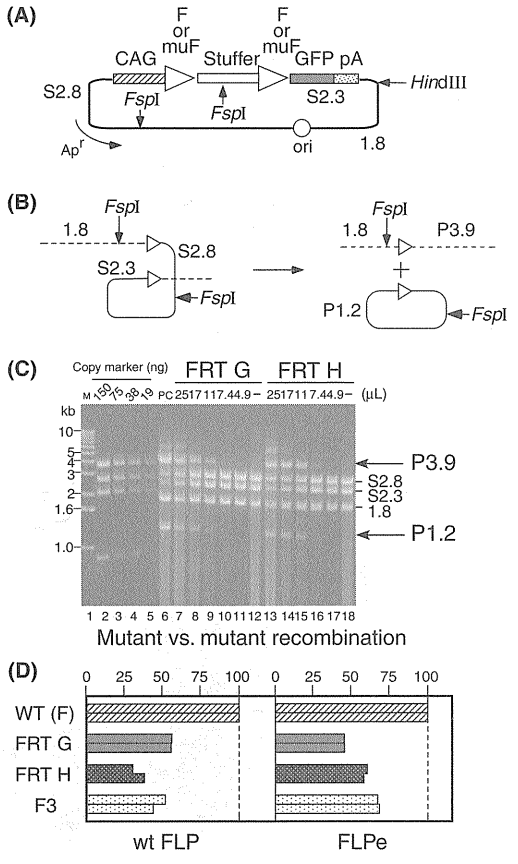

Figure 2 *In vitro* recombination assay using DNA substrates between identical mutant FRTs. (A) Structure of pCAFNFG-based substrate plasmids (F, FRT; muF, mutant FRT; triangle, FRT sequence; CAG, CAG promoter; stuffer, neo gene plus SV40 polyadenylation sequence; pA, rabbit β-globin polyadenylation sequence). (B) Recombination process using pCAFNFG-based, *Hin*dIII-linearized substrate (Open triangle, FRT sequence; S, substrate-derived band; P, product-derived band). (C) Quantification of recombined products using FLPe [M (lane 1), 1-kb ladder marker; PC (lane 6), positive control, i.e. recombination between wt FRTs; P, recombined product; S, unrecombined substrate]. One example of the experiments is shown. (D) Recombination efficiency between identical mutant FRTs. The ratios of efficiency between wt FRTs using wt FLP lysate at 30 °C or FLPe lysate at 37 °C are shown. The measured recombination efficiencies of positive control (recombination between two wt FRTs) were 46.6% for wt FLP at 30 °C and 82.1% for FLPe at 37 °C; the bar chart showed the ratios of efficiency when these recombination efficiencies of positive control were regarded as 100. Experiments in each condition were carried out twice.

In vitro RMCE of Cre/*lox*P 2272 and FLP/mutant FRT

To examine the process of RMCE reactions using Cre and FLP *in vitro*, linear and circular Substrates (S) were prepared (Fig. 3A, top), each of which contained one wt target (denoted T) and one mutant target (denoted mT): for Cre, the former was wt *lox*P and the latter was *lox*P 2272, whereas for wt FLP and FLPe, the former was wt FRT and the latter was mutant FRT G, FRT H, or FRT F3. After the linear

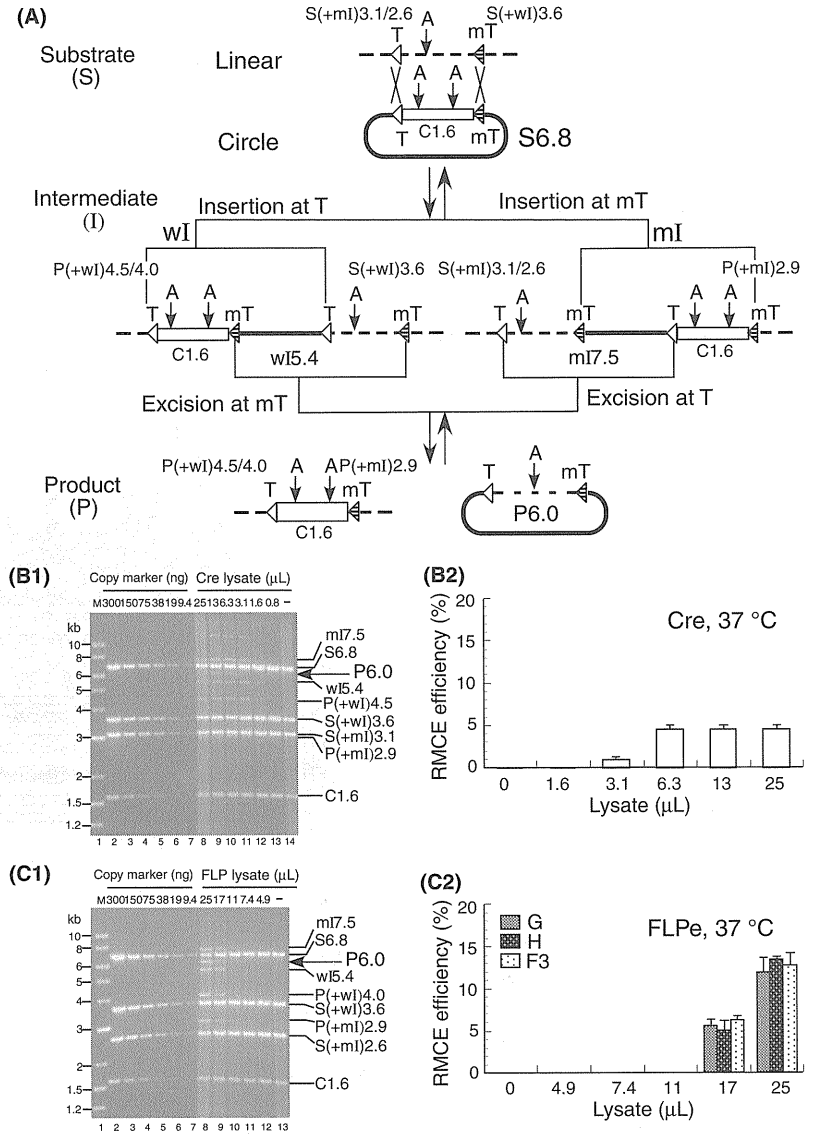

Figure 3 Quantitative recombination assay of *in vitro* RMCE. (A) Recombination process of *in vitro* RMCE [T (target, open triangle), wt *lox*P or wt FRT; mT (mutant target, diagonal triangle), *lox*P 2272, FRT G, FRT H or FRT F3; open rectangle, exchanging range in the circular substrate; A, *Apa*I site; wI, intermediate generated by insertion at wt target; mI, intermediate generated by insertion at mutant target]. (B1) Quantification of recombined products using Cre and *lox*P. *Dra*I-linearized pVCAG-FP15L and circular pVEFZL were reacted (underline shows wt and mutant *lox*Ps) and then digested with *Apa*I [M (lane 1), 1-kb ladder marker; S, substrate; P, product; wI and mI, intermediate generated by recombination between wt *lox*Ps or mutant *lox*Ps, respectively; C, constantly present regardless of recombination]. Parentheses with + such as S(+wI), the bands derived from Substrate or Product (top or bottom of A) but also containing the identical DNA derived from the Intermediate generated by the insertion at T and mT (middle left and light of A). (B2) Recombination efficiency of RMCE product using Cre. The ratio of the intensity of the bands P6.0 in B1 to the total intensity of the Substrate in the negative control (B1, lane 14) is shown. These intensities were judged using copy markers of lanes 2–7. The bars were calculated from the results of three independent experiments. (C1) Quantification of recombined products using FLPe and mutant FRT G. One result for mutant FRT G is presented as a representative example of the three mutant FRTs. The size of the bands of P+wI4.0 and S(+mI)2.6 differed from the corresponding bands in B1 because of the 0.5-kb insertion (see Experimental procedures). All other representations are the same as in B1. (C2) Recombination efficiencies of RMCE products using FLPe. The bands of P6.0 in C1, lanes 7–12, are shown together with those of the Substrate in the negative control in C1, lane 13, for example, are shown. Three independent experiments were carried out for each mutant recombinase.

or circular substrates were mixed and reacted with the recombinase *in vitro* (Lee & Saito 1998; Nakano *et al.* 2001b), two Substrates were produced before recombination (Fig. 3A, top) in addition to two recombined Products (P) (bottom) and two Intermediates (middle) (wI for 'wt-target intermediate' generated by the insertion of a circular substrate into a linear substrate at the target and mI for 'mutant-target intermediate' generated by insertion into a linear substrate at the mutant target). The Intermediate wI (middle left) was produced when the insertion (first recombination) occurred at the wt *lox*P site before the deletion (second recombination). Similarly, an Intermediate mI (middle right) was also produced.

The resulting DNAs were digested with *Apa*I (as shown in Fig. 3A), and the expected bands were shown as the original position and size, such as S6.8, meaning a Substrate-derived 6.8-kb *ApaI* fragment. Among the Substrates, the circular substrate (top, lower) produced a band of S6.8 and a constant band of 1.6 kb (C1.6) from the unchanged part of the circular substrate after recombination. The linear substrate (top, higher) yielded two thick bands: the right band S(+wI)3.6 corresponded to the Substrate-derived 3.6-kb band overlapping a wt-target intermediate (wI)-derived band of the same size. The right band S(+mI)3.1/2.6 corresponded to a Substrate-derived and partly overlapping mI-derived band as described earlier, with a size of 3.1 kb for the Cre experiments and 2.6 kb for the FLP experiments. This difference in size was caused by the pUC backbone with or without the M13 sequence (see Experimental procedures). The wI5.4 and mI7.5 (middle left and right) were intermediate-specific, wI-and mI-derived *Apa*I bands of 5.4 and 7.3 kb, respectively. P(+wI)4.5/4.0 and P(+mI)2.9 (bottom left) were Product-derived bands overlapping intermediates with the same size; P6.0 (bottom right) was a product-specific 6.0-kb band.

An RMCE reaction using Cre with target wt *lox*P and mutant target *lox*P 2272 was performed; the result (Fig. 3B1) produced all the expected Substrates, Intermediates, and Products after *Apa*I digestion, as shown in Fig. 3A (compare all the expected *Apa*I fragments in Fig. 3A with the detected bands in Fig. 3B1; the intensity of the bands is discussed later). Similarly, after the reaction using wt FLP and target FRT G at 30 °C, all the expected bands in Fig. 3A were also detected (Fig. 3C1). These results showed that the scheme for the recombination process involved in RMCE *in vitro* and shown in Fig. 3A was correct.

In the *in vitro* RMCE using Cre (Fig. 3B1), the Substrate-derived bands of 6.8 kb (S6.8) and the overlapped bands of Substrate and Intermediates were all very intense (lanes 8–13; S6.8, S(+wI)3.6 and S(+mI)3.1), whereas the bands of Intermediates, Product, and Product-overlaps were all weak [lanes 8–13; mI7.5, P6.0, wI5.4, P(+wI)4.5 and P(+mI)2.9], indicating that RMCE using Cre was not very effective even when 25 μL of lysate was used (lane 8). Interestingly, the amount of RMCE product using Cre clearly reached a maximum with the addition of 6.3 μL of lysate and then maintained a plateau level (Fig. 3B1, lanes 8–10, P6.0). In contrast, in the *in vitro* RMCE using wt FLP with wt FRT and FRT G at 30 °C (Fig. 3C1), amounts of Intermediates, Product, and Product-overlaps rapidly increased and remarkably reached much higher level than Cre [Fig. 3C1, lanes 9 and 10; mI7.5, P6.0, wI5.4, P(+wI)4.0 and P(+mI)2.9: compare with the corresponding bands of Cre in Fig. 3B1, lanes 9 and 10], indicating that RMCE using wt FLP was much more efficient than RMCE using Cre. Because the product band P6.0 continued to increase in Fig. 3C1, from lanes 8 to 10, showing that the RMCE level using wt FLP did not reach a plateau within this experimental range. Then, experiments using wt FLP at 30 °C with wt FRT and FRT H/FRT F3 were carried out, and the results were very similar to those shown in Fig. 3C1 (photograph data are not shown, bar charts were shown in Fig. S1 in Supporting Information). We carried out identical experiments using FLPe at 37 °C with wt FRT and each of the three FRT mutants and the results were again very similar to those shown in Fig. 3C1 (photos not shown but bar charts were shown later). Thus, when using wt FLP and FLPe with wt FRT and each of these three mutant FRTs, the RMCE efficiency was always much higher than that using Cre with wt *lox*P and *lox*P 2272.

To quantify the RMCE efficiency using Cre, wt FLP and FLPe, the intensities of the product bands of P6.0 were measured based on those of the bands in agarose gels electrophoresed in parallel (Fig. 3B1, C1, lanes 2–7). For Cre, the RMCE efficiency reached a plateau of 4.6% (Fig. 3B2). For FLPe, the maximum efficiency observed was 12–13%, and no significant difference was observed between the three FRT mutants (Fig. 3C2). The results were very similar to those for wt FLP with wt FRT and the three mutants, and the efficiency was approximately 13–14% (data not shown, but a photograph showing the data for wt FLP with wt FRT and FRT G is shown

as Fig. 3C1). When using a linear substrate or a circular substrate alone, no bands except for the substrate-derived band were observed (data not shown).

Cre and FLPe enzymes in the lysates were produced by infection of AdVs expressing the recombinases under the control of CAG promoter to 293 cells in the same manner. To compare levels of expressed Cre and FLPe RNAs in the lysates, total RNA was extracted from the lysates used in the aforementioned experiments, and the specific RNA of these recombinases was quantified using real-time PCR with probes detecting the common 3′-noncoding polyadenylation sequence. The results showed that the ratio of RNA levels in the lysates of Cre to FLPe used in these experiments was 1:1.15 ± 0.05, showing that the amounts of these RNAs were similar. Because FLPe is thermostable, the amounts of recombinases present in the lysates were expected also similar. Thus, the reason why RMCE efficiencies were different was not because of the difference of their amounts in the lysates but probably attributed to that of the nature between Cre and FLPe.

Efficient AdV production using hFLPe RMCE

The result that the RMCE efficiency of FLPe was higher than that of Cre prompted us to examine the efficiencies of AdV production using RMCE, a method we previously developed using Cre (Nakano *et al.* 2005), and to examine which recombinase is more efficient in RMCE. To develop a method for AdV production using FLP RMCE, the generation of a 293 cell line highly expressing FLPe was necessary. Thus, we used genes of not only FLPe but also the hFLPe (Kondo *et al.* 2009), an improved version of the FLPe gene in which the codon usage has been changed to that used in humans and that produces more FLPe enzyme. The 293 cells were transfected with plasmids producing FLPe under the control of the CAG promoter (Niwa *et al.* 1991) and the neo gene under control of the EF1α promoter. After drug selection, 293 cell clones expressing high-level of FLPe RNA were identified (data not shown) and listed in Table 1. The cell line 293hde12 was identified expressing the highest amount of FLPe protein. To compare the RMCE efficiency of AdV production using FLP with that using Cre, the donor plasmid and the recipient virus in this study were constructed identically to those used by Nakano *et al.* (2005), except for the use of FLPe, wt FRT (F), mutant FRT G, and FRT H in Fig. 1A, instead of Cre, wt *lox*P (L), and mutant *lox*P (V), so that the recipient virus AxGEFLacZF19F with the donor plasmid pUGCAGFP19F and AxHEFLacZF19F with pUHCAGFP19F exactly corresponded to AxVEFLacZL19L and pUVCAGFP19L reported by Nakano *et al.* (2005), respectively.

Table 1 Recombinase-mediated cassette exchange efficiency of adenovirus vector (AdV) production for FLP-expressing 293 cell lines using the first stock

Cell line	FLP	AdV production efficiency (%)
293hde12*	hFLPe	52
hde24	hFLPe	41
E18	FLPe	38
E11	FLPe	30

*The same cell line used for the experiment of Fig. 4C, G 1st. The amount of AdV-transduced gene of interest was obtained by subtracting that of ApR (carryover donor plasmid) from that of GFP.

The production of purpose vector receiving the gene of interest (gray box in Fig. 4A, bottom), the GFP gene under the control of the CAG promoter, initially presents in the donor plasmid (top right), was carried out as follows. In the donor plasmid (top right), the gene of interest plus the adenoviral packaging sequence (Ψ) was located between FRT G or FRT H and wt FRT (F). Meanwhile, in the recipient virus (top left), a replaced gene (white box; *lac*Z gene under the control of EF1α promoter) was located between the FRT G or FRT H and wt FRT and Ψ were located between the left and right wt FRTs (Fig. 4A, top left). Then, the plasmid and virus were transfected and infected to FLPe-expressing 293 cells. First, the excision of Ψ was occurred from the viral genome; a recipient-virus genome lacking Ψ cannot be packaged into the viral shell (middle left). Second, an RMCE reaction between the Ψ-less recipient virus genome and the donor plasmid (middle left) produced a viral genome containing both Ψ and the gene of interest, being able to be packaged into a viral shell. In this manner, a purpose vector containing the gene of interest was produced (Fig. 4A, bottom). The 293hde12 cells were transfected with pUGCAGFP19F and infected with AxGEFLacZF19F at an MOI of 1. The first viral stock was prepared and then used to infect 293hde12 cells to prepare a second viral stock to obtain the purpose vector of AxGCAGFP19F. The first and second stocks of AxHCAGFP19F were prepared in a similar manner. All the conditions for preparing the viral stocks were identical to those used by Nakano *et al.* (2005).

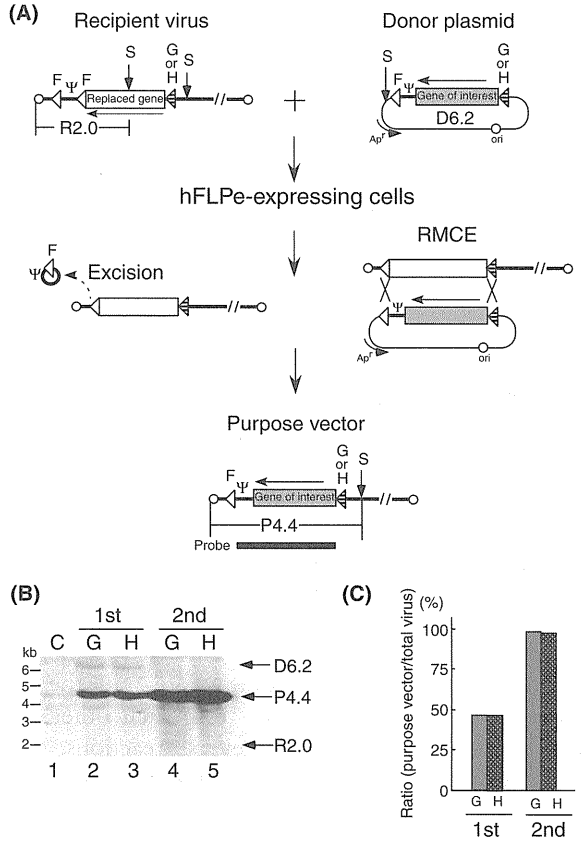

Figure 4 Production of first-generation adenovirus vector (AdV) by FLPe-mediated RMCE. (A) Strategy for the generation of adenoviral vectors using the RMCE reaction. Structure of recipient virus AxGEFLacZF19F or AxHEFLacZF19F, donor plasmid pUGCAGFP19F or pUHCAGFP19F, and purpose vector AxGCAGFP19F or AxHCAGFP19F is shown [F, wt FRT; G, FRT G; H, FRT H; Ψ, adenovirus packaging sequence; replaced gene, *lac*Z gene under control of EF1α promoter; gene of interest, GFP gene under the control of CAG promoter as an example; S, *Sac*I site; R2.0, D6.2, and P4.4, recipient virus-, donor plasmid-, and purpose vector-derived bands of 2.0, 6.2, and 4.4 kb, respectively]. (B) Southern analysis of total DNA extracted from infected CV-1 cells. C, control uninfected cells. The probe is 'Ψ + gene of interest' shown in the bottom of (A). The other presentations are the same as above. (C) Production efficiency of AdV. Ratio of the purpose vector to the total virus (purpose vector + recipient virus) transduced to the CV-1 cells was shown. The data of Cre in this figure were those of Nakano *et al.* (2005). Experiments including data using other cells expressing high-level of FLP were carried out six times. Representative results are shown.

To examine the ratio between the donor plasmid and the purpose vector, CV-1 cells were infected with the first and second viral stocks. The cell DNA was extracted, digested with *Sac*I, and used in Southern analyses. Fig. 4B showed that even in the first stock of both RMCEs using wt FRT and FRT G/FRT H, much purpose virus was detected together with carryover donor plasmid (lanes 2 and 3, P4.4 and D6.2). The band of the recipient virus (R2.0) was not seen in this gel, probably because the region of homology with the probe (Ψ only) was relatively short (Fig. 4A).

To estimate the percentage of the purpose vector per total vector, CV-1 cells were infected with aliquots of the first and second stocks and infected total cell DNA was extracted. The GFP probes detect both AdV-transduced gene of interest and the carryover donor DNA present when infected using the first stock. Densitometry of the bands of D6.2 and P4.4 in Fig. 4B showed that the latter accounted for approximately 10% when using the first stock and was background level using the second stock. Then, the amounts of AdV-transduced gene of interest (approximately 90% using the first stock) and the total adenovirus genome were measured using real-time PCR (Fig. 4C). The percentages in RMCE when using FLPe with wt FRT and FRT G/FRT H were apparently identical and approximately 45% in the first stock; interestingly, these percentages were clearly higher than 25% when using Cre with wt *lox*P and *lox*P 2272 reported by Nakano *et al.* (2005). However, in the second stock, the percentage reached approximately 98% using FLPe with wt FRT and FRT G/FRT H, which were similar to the reported percentage of 85% using Cre (Nakano *et al.* 2005). The CV-1 cells infected with AdV of the second stocks using FRT G and FRT H showed expected GFP fluorescence observed by microscopy and FACS (data not shown), which cannot distinguish with results using the authentic AdV-expressing GFP. These results suggested that, when 293hde12 cells and 293FNCre cells were used, FLPe with wt FRT and FRT G/FRT H was more efficient than Cre with wt *lox*P and *lox*P 2272 at the first passage of AdV production using RMCE.

To examine the efficiency of AdV production in the FLPe-expressing cells listed in Table 1, cells were both infected with AxGEFZF19F and transfected with pUGCAGFP19F, and total cell DNA was prepared as above and used for real-time PCR. The amounts of not only GFP and lacZ genes but also ampicillin-resistance (ApR) gene in the carryover donor plasmid were measured instead of performing Southern analysis, and the amounts of AdV-transduced gene of interest and the total adenovirus genome were

calculated. As shown in Table 1, besides 293hde12, three cell lines also showed efficiencies of 41–30%, which were higher than those of 25% using Cre in the study by Nakano *et al.* Although these results were not a direct comparison, they suggested that FLPe was possibly more efficient than Cre to obtain the cell lines that supported more efficient AdV production using RMCE.

Discussion

In this paper, we reported that (i) mutant FRTs, i.e. FRT G, FRT H, and FRT F3, exhibited an efficiency of 50–70% in conjunction with wt FRT in mutant-vs.-mutant recombination using wt FLP and FLPe; (ii) in an *in vitro* RMCE assay, Cre reached a plateau of approximately 5%, whereas FLP reached 12–13%; and (iii) in an AdV production system using RMCE, FLPe appeared to be more effective than Cre. The results of (ii) and (iii) were interesting because Cre is generally considered to be more efficient than or equal to FLPe. Further studies are needed to determine whether the observation described here can be generalized or not. However, it should be noted that extremely high level of Cre and FLPe was supplied in the *in vitro* experiments using AdV vector production system; when lower levels of the recombinases are used, such as 3.1 and 6.3 μL of Cre lysate and 7.4 and 11 μL FLPe (Fig. 3B2,C2), the RMCE efficiency of Cre was high whereas that of FLPe was still undetectable. Thus, one possibility is that only in a very high concentration, FLPe may be more efficient than Cre in RMCE reaction. Buchholz *et al.* (1996) showed that at each optimal temperature, wt FLP is more efficient than Cre in *in vitro* assay using the system of reticulocyte lysate. Although the *in vitro* system is different, their result may be consistent with our observation in *in vitro* RMCE assay at high concentration of the recombinases. No significant difference of RMCE efficiency was observed among three FRT mutants of FRT G, FRT H, and FRT F3 in *in vitro* (Fig. 3C2), suggesting that these FRT mutants are equally useful for RMCE. However, the recombination efficiency of mutant-vs.-mutant seemed significantly different (Fig. 2D, right). The reason of this apparent disagreement is unclear but may be related that, whereas the latter is an intramolecular reaction, the former is intermolecular reactions involving two molecules of a linear and a circle. We want to point out that we choose FRT G and FRT H because these two mutant FRTs may possibly be used simultaneously as the central nucleotides differ from each other by two nucleotides at the same positions (see Fig. 1A), based on the experiences identifying mutant *lox*Ps 2272 and 5171 (Lee & Saito 1998). The *lox*P 2272 has been used in many studies; however, note that it was incorrectly described in the study by Siegel *et al.* (2001), FEBS Letters. Our previous work (Lee & Saito 1998) indicated that the incorrect mutant *lox*P showed only a low recombination efficiency. The correct central eight bases of *lox*P 2272 are GGATACTT, i.e. complementary to AAGTATCC (underlines show the mutated nucleotides) (Fig. 1B).

As described previously, in our *in vitro* assay, the amount of RMCE product (P) using Cre reached a maximum level and did not increase with the addition of more enzyme in contrast to the case of FLPs. One possible explanation for the plateau using Cre was that a reverse RMCE reaction occurred with Cre but not with the FLPs in a high concentration. That is, the processed products and intermediates in the Cre reaction may still be able to attach together and function as a reverse reaction, whereas in the FLP reaction, they may come apart from each other, preventing their involvement in reverse reactions. Consistent with this hypothesis, under the conditions used here and in our previous work, the Cre recombination efficiency *in vitro* between the two wt *lox*Ps reached a plateau level of approximately 60% (Abremski *et al.* 1983; Lee & Saito 1998), whereas the FLPe efficiency *in vitro* between the two wt FRTs reached approximately 80% and then showed a plateau (Kondo *et al.* 2009). The former level was nearer to 50% than the latter, consistent with the notion that Cre recombination may be reversible. In addition, because the RMCE reaction *in vitro* is not a single step but a double, small differences in the reverse reaction may have a large effect. The difference might be related to the fact that the roles of Cre and FLP completely differ in the organism where they belong; FLP inverts a DNA sequence in 2-micron plasmid, and hence, the recombinated products are still connected with in a plasmid *in vivo* and never become apart; in contrast, in the bacteriophage P1, Cre resolves a dimer of two monomers of the circular genome of its plasmid form. However, the present study described here in a very high concentration of enzymes seems not sufficient to interpret this enzymatic difference.

We also observed that in the production of AdV using RMCE, the FLPs once again appeared to be more efficient than Cre; thus, an identical or similar mechanism to that observed in the *in vitro*

experiments might also occur during AdV production. If some reverse reaction of Cre occurs, it is perhaps one reason of low efficiency of Cre reaction; in *in vitro* RMCE, double steps of reactions are necessary, and in AdV production, one step of excision plus double step of reactions is serially needed (Figs 3A and 4A). We also observed that recombination efficiency of Cre in the recipient virus using the cell line 293FNCre remained at approximately 80% (Nakano *et al.* 2005), whereas that of hFLPe using the cell line 293hde12 was approximately 95% (S. Kondo, unpublished data). However, as for the cell lines, another essential reason for the low activity of Cre should be considered: high levels of Cre expression can cause cytotoxicity (Loonstra *et al.* 2001; Pfeifer *et al.* 2001; Baba *et al.* 2005); hence, a cell line expressing a high level of Cre would be selected out by a screening procedure. In fact, 293hde12 grows much better to culture than 293FNCre (Y. Kanegae, unpublished data). However, a 293 cell line has been reported that expresses very high levels of Cre yet can achieve nearly 100% recombination (Palmer & Ng 2003). We observed that a small amount of carryover donor plasmid was detected in the first passage, whereas more carryover plasmid was observed in the study by Nakano *et al.* (2005). The amount of carryover DNA varied from experiment to experiment and may be attributed to the difference of cell nature or to that of washing conditions.

The methods of AdV production using FLPe described here and that using Cre (Nakano *et al.* 2005) differ from all other methods producing AdV currently available. They must deal with a very large plasmid or cosmid because they contain most of adenoviral genome, which amounts to more than 30 kb. In contrast, the method described here and in the study by Nakano *et al.* (2005) uses only a small donor plasmid containing a DNA fragment, such as an expression unit to be transferred into an AdV. As shown in Fig. 4D, after two passages in 293hde12 cells, an almost pure viral stock was obtained when using FLPe. However, AdV production efficiency of FLPe with wt FRT and FRT G/FRT H was approximately double than that of Cre with wt *lox*P and *lox*P 2272 at the first passage. This feature is important when the production method is applied for high-throughput production and for AdV cDNA library followed by subsequent screening of cDNA-expressing AdVs, because higher production efficiency is crucial at the step of first passage. Another important difference between the AdV production systems of Cre and FLPe is that, as stated previously, the FLPe-expressing 293 cells, 293hde12, are much easier to culture than Cre-expressing 293 cells, 293FNCre (Nakano *et al.* 2005).

In conclusion, we observed that, when sufficient amount of FLPe was supplied, the RMCE efficiency of FLPe was higher than that of Cre *in vitro,* because the RMCE reaction of Cre reached a plateau level. Moreover, FLPe was again more efficient in AdV production. Thus, as for the RMCE reaction, Cre was not necessarily more efficient than FLPe. The study described here offers valuable information when choosing a recombinase for a particular purpose using RMCE. The donor plasmid cassette pUGp19F or its improved version pUGan19F and PUGna19F, recipient virus AxGEFLacZF19F, and the cell line 293hde12 are available on a collaborative basis and will be from RIKEN Bioresources Bank (http://dna.brc.riken.jp/index.html).

Experimental procedures

Cells and viruses

The human embryonic kidney cell line 293 (Graham *et al.* 1977) and the monkey kidney cell line CV-1 were cultured in DMEM supplemented with 10% fetal calf serum (FCS). The 293 cells constitutively express adenoviral E1 genes and support the replication of E1-substituted AdVs. 293FNCre (Nakano *et al.* 2005) and 293hde12 are 293 cells constitutively expressing Cre and FLPe, respectively, and these cells were cultured in DMEM supplemented with 10% FCS plus geneticin (0.75 mg/mL). After infection with recombinase-expressing AdVs, the cells were maintained in DMEM supplemented with 5% FCS without geneticin. The detailed characterization of 293hde12 cells will be presented elsewhere. For AdV production using RMCE method of Cre with *lox*P 2272, the donor plasmid pUVCAGFP19L and recipient virus AxVEFZL19L were described previously (Nakano *et al.* 2005). For AdV production using RMCE and mutant FRT, the donor plasmids pUGCAGFP19F and pUHCAGFP19F and the recipient virus AxGEFZF19F and AxHEFZF19F are identical to pUVCAGFP19L and AxVEFZL19L (Nakano *et al.* 2005), except that wt *lox*P and *lox*P 2272 were replaced by wt FRT and FRT G or FRT H, respectively (in this paper, wt FRT, FRT G, FRT H, FRT F3, wt *lox*P, and *lox*P 2272 are used to describe the plasmids and the AdVs are denoted as F, G, H, F3, L, and V, respectively).

Preparation of recombinase lysates for *in vitro* reaction

The wt FLP and FLPe were prepared as a lysate of 293 cells infected with AdV expressing the recombinase under the control of CAG promoter (Nakano *et al.* 2001a,b; Kondo

et al. 2009). The FLPe gene used for AdV expression was the original FLPe gene (Genebridges), but an artificially attached nuclear localization sequence (NLS) was removed for accurate comparison with wt FLP. Briefly, 2×10^7 of 293 cells were infected with AxCAFLP and AxCAFLPe at a multiplicity of infection (MOI) of 75 and 5, respectively. Twenty-two hours later, the cells were corrected by centrifugation at 185 *g* for 5 min at 4 °C. The cell pellet was washed twice with PBS(−) and suspended in 1 mL of FLP storage buffer (Meyer-Leon *et al.* 1984) [10% glycerol, 20 mM Tris–HCl (pH 7.5), 300 mM NaCl, 1 mM EDTA, and 0.02 mM PMSF]. The cell suspension was then sonicated for 3 min (six cycles, 30 s each), using Biorupter II (CosmoBio, Tokyo, Japan) at maximum power (200 W), and was then immediately centrifuged at 12 096 *g* for 20 min at 4 °C. The supernatant was stored at −80 °C. The Cre used in this paper was NCre, which was tagged with NLS (Lee & Saito 1998). The Cre lysate was prepared using a previously described method (Lee & Saito 1998; Kondo *et al.* 2003), which was identical to the above for FLPe except for the virus (AxCANCre), MOI of 5 and the composition of the storage buffer (Cre storage buffer (Anton & Graham 1995): 50% glycerol, 20 mM Tris–HCl (pH7.5), 300 mM NaCl, and 1 mM EDTA without PMSF).

Substrate plasmids in the *in vitro* reaction

pCAFNFG (Fig. 2A), the substrate used to examine mutant-vs.-mutant recombination and wt FRT-vs.-mutant recombination to detect leakage, has been described previously (Nakano *et al.* 2001b). pCAGNGG, pCAHNHG, and pCAF3NF3G were identical to pCAFNFG except that two wt FRTs were replaced by two FRTs G, FRTs H, and FRTs F3, respectively. Similarly, pCAFNGG, pCAFNHG, and pCAFNF3G were identical to pCAFNFG except that the second wt FRT was replaced by FRT G, FRT H, and FRT F3, respectively. For the *in vitro* RMCE reaction using Cre, the linear substrate was *Dra*III-linearized pUVCAGFP15L, which is identical to pUVCAGFP19L (Nakano *et al.* 2005) except that the position of one wt *lox*P is not at 191 nt from the left end of the adenovirus 5 genome but at 143 nt; the backbone of this plasmid is pUC119, which contains a 0.5-kb M13 sequence. The circular substrate was pVEFZL, which contains *lox*P 2272, the EF1α promoter, the *Lac*Z gene, and wt *lox*P, in this order. For the *in vitro* RMCE reaction using FLP, the linear substrate was *Sac*I-digested pUFCAGFP15G, pUFCAGFP15H, or pUFCAGFP15F3; the backbones of these plasmids are derived from pUC19, which is identical to the above corresponding linear substrate for Cre, except that it lacks the M13 origin sequence, whereas the structure of the insert flanked with recombinase-targets was identical between these three FLP target plasmids and pUVCAGFP15L. The circular substrate was pGEFZF, pHEFZF, or pF3EFZF, and the structures were identical to those of the above-described pVEFZL, except for the corresponding recombinase targets.

In vitro reaction for mutant-vs.-mutant and RMCE recombination

The *in vitro* recombination assay for the mutant-vs.-mutant recombination of each FRT was carried out as described previously (Nakano *et al.* 2001b). Briefly, for wt FLP and FLPe, the reaction was started by mixing 1 μg of *Hin*dIII-linearized substrate with a lysate volume of 4.9–25 μL and was then incubated for 30 min at 30 or 37 °C in a 50-μL volume of the FLP reaction buffer [25 mM Tris–HCl (pH7.5), 10 mM $MgCl_2$, and 5 mM DTT]. The reaction was terminated by the addition of 100 μL of 7 M urea mixture [7 M urea, 350 mM NaCl, 10 mM Tris–HCl (pH7.5), 10 mM EDTA, and 1% SDS] with 50 μL of distilled water. The mixture was extracted twice with phenol/chloroform, followed by two cycles of chloroform extraction and ethanol precipitation. The recovered DNA was then digested with *Fsp*I, and the DNA digests were detected using ethidium bromide staining after agarose gel electrophoresis. The recombination efficiency was calculated by quantifying the density of the product bands of 1.2 kb and the constant bands of 1.8 kb on the photograph based on the densities of the copy-marker DNA digests run on the same gel, as described previously (Nakano *et al.* 2001b). The copy-marker DNA is pCALNLZ plasmid of 9.22kb (Kanegae *et al.* 1996). The *Eco*RI-linearized pCALNLZ was digested with *Nco*I produced bands of 3.67, 2.62, 2.01 and 0.92 kb, which correspond to 39.9%, 28.4%, 21.8%, and 10.0% of pCALNLZ, respectively.

The *in vitro* recombination assay of RMCE for Cre between wt *lox*P and *lox*P 2272 was carried out using an identical protocol to that described previously except that a mixture of 1.2 μg of *Dra*III-linearized pUVCAGFP15L and 1.5 μg of circle pVEFZL was reacted with Cre lysate and digested with *Apa*I. For the wt FLP and the FLPe between wt FRT and FRT G, FRT H, or FRT F3, an identical protocol was used except that a mixture of 1.1 μg of *Sac*I-linearized and 1.5 μg (the same mol) of circle pGEFZF, pHEFZF, or pF3EFZF substrates, respectively, was reacted with a lysate of wt FLP or FLPe and digested with *Apa*I. The recombination efficiency was calculated by quantifying the density of the product bands of 6.0 kb (P6.0) and of the constant bands of 1.6 kb (C1.6).

Quantitative real-time PCR

To compare the amounts of expressed RNA of Cre and FLPe, the total RNA was extracted from the lysates used in *in vitro* experiments. The 3′-noncoding regions of these RNAs are common and derived from rabbit–globin poly(A) sequence. Thus, the specific RNA of the recombinase was able to be measured and compared using the same set of primers located within the poly(A) sequence (GpA promers: forward primer, 5′-TCA GGT GCA GGC TGC CTA T-3′; reverse primer, 5′-GGA AAA AGA TCT CAG TGG TAT TTG TGA-3′, and TaqMan probe, 5′-FAM-CTG GTG TGG CCA ATG CCC TGG -TAMRA-3′). From

the total RNA, the amounts of the recombinase RNA and 18S-rRNA (correction standard) were quantified using reverse-transcription and real-time PCR (Applied Biosystems Prism 7000), and the ratio of the recombinase RNA to 18S-rRNA was obtained. Then, the ratio of the recombinase RNA level between Cre and FLPe lysates was calculated.

Production of adenovirus vector by RMCE

The method for the production of AdV by RMCE using FLPe was the same as that described previously for Cre (Nakano *et al.* 2005): FRT G or FRT H, the FLPe-expressing cells, 293hde12, the recipient virus AxGEFZF19F or AxHEFZF19F, and the donor plasmid pUGCAGFP19F or pUHCAGFP19F corresponded to, the wt *lox*P, 293FNCre cells, AxVEFZL19L and pUVCAGFP19L, respectively. Briefly, the FLPe-expressing 293hde12 cells were infected with the recipient virus AxGEFZF19F or AxHEFZF19F at about an MOI of 1, when complete cytopathic effect is observed 4 days after infection, and were cultured in a 6-well plate for 1 h, followed immediately by the transfection of the donor plasmid pUGCAGFP19F or pUHCAGFP19F at a density of 3.0 μg per well using TransFast (Promega). When a viral cytopathic effect was clearly observed, the cells were harvested together with the medium (approximately 1.5 mL per well). The cell suspension was then sonicated for 3 min (six cycles, 30 s each) using a Bioruptor II sonicator (CosmoBio) at maximum power (200 W) and centrifuged at 1900 *g* for 5 min at 4 °C using a microcentrifuge. The supernatant was stored at −80 °C as a 'first virus stock'. To enrich the purpose vector by eliminating the residual recipient virus, 293hde12 cells were infected with 50 μL of the first viral stock, and the second viral stock was prepared as described earlier.

Southern blot analysis

To detect the 'infectious virus' DNA of the purpose vector and the residual recipient viruses, the CV-1 cells were infected with the virus stocks at 100 μL per 6-cm dish. Twenty-four hours later, the total DNA-containing viral genome was prepared from the dish with the method described by Saito *et al.* (1985). After *Sac*I digestion, 20 μg of the DNA was electrophoresed on a 0.8% agarose gel at 35 V for 17 h. Before alkaline treatment, the gel was exposed to 0.1 N HCl for partial depurination (Saito *et al.* 1989), and the DNA was then transferred to a Hybond-N nylon membrane (Amersham Biosciences) using the capillary-transfer method. The specific DNA was detected with a DIG DNA Labeling and Detection Kit (Roche Diagnostics). A 3.4-kb *Kpn*I-*Xho*I fragment of the adenoviral packaging sequence (Ψ) and the GFP gene was labeled with digoxigenin-UTP as probes (Fig. 4A), and specific DNAs were detected by autoradiography using chemiluminescence of CDP-Star (Roche Diagnostics).

Measurement of the ratio of the purpose vector to the recipient viruses

The ratio of the produced purpose vector to the residual recipient viruses was measured as described previously (Nakano *et al.* 2005); the total DNA was extracted from CV-1 cells infected with viruses of each virus stock and was subjected to quantitative real-time PCR. TaqMan primers and probes specific for the GFP gene in the purpose vector and specific for the *lac*Z gene in the recipient virus are described in the study by Nakano *et al.* (2005). The primers and probe for ApR gene are the following: forward primer, 5′-CGC GGT ATT ATC CCG TGT TG-3′; reverse primer, 5′-CAA CCA AGT CAT TCT GAG AAT AGT GTA TG-3′; and TaqMan probe, 5′-FAM- CGC CGG GCA AGA GCA ACT CG-TAMRA-3′. The difference in the detection efficiency between GFP, *lac*Z, and ApR genes was corrected using the control plasmid pEFVGV-CALNLZ (Kondo *et al.* 2003), containing GFP, *lac*Z, and ApR genes on the same plasmid.

Acknowledgements

This work was supported by a grant from the Ministry of Education, Culture, Sports, Science and Technology, Japan, to IS. We thank Ms. E. Kondo and Ms. M. Terashima for excellent secretarial assistance and technical support, respectively.

References

Abremski, K., Hoess, R. & Sternberg, N. (1983) Studies on the properties of P1 site-specific recombination: evidence for topologically unlinked products following recombination. *Cell* **32**, 1301–1311.

Akopian, A. & Marshall Stark, W. (2005) Site-specific DNA recombinases as instruments for genomic surgery. *Adv. Genet.* **55**, 1–23.

Andreas, S., Schwenk, F., Kuter-Luks, B., Faust, N. & Kuhn, R. (2002) Enhanced efficiency through nuclear localization signal fusion on phage PhiC31-integrase: activity comparison with Cre and FLPe recombinase in mammalian cells. *Nucleic Acids Res.* **30**, 2299–2306.

Anton, M. & Graham, F.L. (1995) Site-specific recombination mediated by an adenovirus vector expressing the Cre recombinase protein: a molecular switch for control of gene expression. *J. Virol.* **69**, 4600–4606.

Baba, Y., Nakano, M., Yamada, Y., Saito, I. & Kanegae, Y. (2005) Practical range of effective dose for Cre recombinase-expressing recombinant adenovirus without cell toxicity in mammalian cells. *Microbiol. Immunol.* **49**, 559–570.

Beard, C., Hochedlinger, K., Plath, K., Wutz, A. & Jaenisch, R. (2006) Efficient method to generate single-copy transgenic mice by site-specific integration in embryonic stem cells. *Genesis* **44**, 23–28.

Belteki, G., Gertsenstein, M., Ow, D.W. & Nagy, A. (2003) Site-specific cassette exchange and germline transmission

with mouse ES cells expressing phiC31 integrase. *Nat. Biotechnol.* **21**, 321–324.

Birling, M.C., Gofflot, F. & Warot, X. (2009) Site-specific recombinases for manipulation of the mouse genome. *Methods Mol. Biol.* **561**, 245–263.

Bischof, J. & Basler, K. (2008) Recombinases and their use in gene activation, gene inactivation, and transgenesis. *Methods Mol. Biol.* **420**, 175–195.

Buchholz, F., Angrand, P.O. & Stewart, A.F. (1998) Improved properties of FLP recombinase evolved by cycling mutagenesis. *Nat. Biotechnol.* **16**, 657–662.

Buchholz, F., Ringrose, L., Angrand, P.O., Rossi, F. & Stewart, A.F. (1996) Different thermostabilities of FLP and Cre recombinases: implication for applied site-specific recombination. *Nucleic Acids Res.* **24**, 4256–4262.

Bucholtz, F. (2008) Principles of site-specific recombinase (SSR) technology. *J. Vis. Exp.* **15**, 718. doi:1.03791/718.

Farley, F.W., Soriano, P., Steffen, L.S. & Dymecki, S.M. (2000) Widespread recombinase expression using FLPeR (flipper) mice. *Genesis* **28**, 106–110.

Graham, F.L., Smiley, J., Russell, W.C. & Nairn, R. (1977) Characteristics of a human cell line transformed by DNA from human adenovirus type 5. *J. Gen. Virol.* **36**, 59–74.

Grindley, N.D., Whiteson, K.L. & Rice, P.A. (2006) Mechanisms of site-specific recombination. *Annu. Rev. Biochem.* **75**, 567–605.

Kanegae, Y., Takamori, K., Sato, Y., Lee, G., Nakai, M. & Saito, I. (1996) Efficient gene activation system on mammalian cell chromosomes using recombinant adenovirus producing Cre recombinase. *Gene* **181**, 207–212.

Kondo, S., Okuda, A., Sato, H., Tachikawa, N., Terashima, M., Kanegae, Y. & Saito, I. (2003) Simultaneous on/off regulation of transgenes located on a mammalian chromosome with Cre-expressing adenovirus and a mutant *lox*P. *Nucleic Acids Res.* **31**, e76.

Kondo, S., Takata, Y., Nakano, M., Saito, I. & Kanegae, Y. (2009) Activities of various FLP recombinases expressed by adenovirus vectors in mammalian cells. *J. Mol. Biol.* **390**, 221–230.

Lee, G. & Saito, I. (1998) Role of nucleotide sequences of *lox*P spacer region in Cre-mediated recombination. *Gene* **216**, 55–65.

Loonstra, A., Vooijs, M., Beverloo, H.B., Allak, B.A., van Drunen, E., Kanaar, R., Berns, A. & Jonkers, J. (2001) Growth inhibition and DNA damage induced by Cre recombinase in mammalian cells. *Proc. Natl Acad. Sci. USA* **98**, 9209–9214.

Meyer-Leon, L., Senecoff, J.F., Bruckner, R.C. & Cox, M.M. (1984) Site-specific genetic recombination promoted by the FLP protein of the yeast 2-micron plasmid *in vitro*. *Cold Spring Harb. Symp. Quant. Biol.* **49**, 797–804.

Nakano, M., Ishimura, M., Chiba, J., Kanegae, Y. & Saito, I. (2001a) DNA substrates influence the recombination efficiency mediated by FLP recombinase expressed in mammalian cells. *Microbiol. Immunol.* **45**, 657–665.

Nakano, M., Odaka, K., Ishimura, M., Kondo, S., Tachikawa, N., Chiba, J., Kanegae, Y. & Saito, I. (2001b) Efficient gene activation in cultured mammalian cells mediated by FLP recombinase-expressing recombinant adenovirus. *Nucleic Acids Res.* **29**, E40.

Nakano, M., Odaka, K., Takahashi, Y., Ishimura, M., Saito, I. & Kanegae, Y. (2005) Production of viral vectors using recombinase-mediated cassette exchange. *Nucleic Acids Res.* **33**, e76.

Niwa, H., Yamamura, K. & Miyazaki, J. (1991) Efficient selection for high-expression transfectants with a novel eukaryotic vector. *Gene* **108**, 193–199.

Oumard, A., Qiao, J., Jostock, T., Li, J. & Bode, J. (2006) Recommended method for chromosome exploitation: RMCE-based cassette-exchange systems in animal cell biotechnology. *Cytotechnology* **50**, 93–108.

Palmer, D. & Ng, P. (2003) Improved system for helper-dependent adenoviral vector production. *Mol. Ther.* **8**, 846–852.

Pfeifer, A., Brandon, E.P., Kootstra, N., Gage, F.H. & Verma, I.M. (2001) Delivery of the Cre recombinase by a self-deleting lentiviral vector: efficient gene targeting *in vivo*. *Proc. Natl Acad. Sci. USA* **98**, 11450–11455.

Rodriguez, C.I., Buchholz, F., Galloway, J., Sequerra, R., Kasper, J., Ayala, R., Stewart, A.F. & Dymecki, S.M. (2000) High-efficiency deleter mice show that FLPe is an alternative to Cre-*lox*P. *Nat. Genet.* **25**, 139–140.

Saito, I., Groves, R., Giulotto, E., Rolfe, M. & Stark, G.R. (1989) Evolution and stability of chromosomal DNA coamplified with the CAD gene. *Mol. Cell. Biol.* **9**, 2445–2452.

Saito, I., Oya, Y., Yamamoto, K., Yuasa, T. & Shimojo, H. (1985) Construction of nondefective adenovirus type 5 bearing a 2.8-kilobase hepatitis B virus DNA near the right end of its genome. *J. Virol.* **54**, 711–719.

Schaft, J., Ashery-Padan, R., van der Hoeven, F., Gruss, P. & Stewart, A.F. (2001) Efficient FLP recombination in mouse ES cells and oocytes. *Genesis* **31**, 6–10.

Schlake, T. & Bode, J. (1994) Use of mutated FLP recognition target (FRT) sites for the exchange of expression cassettes at defined chromosomal loci. *Biochemistry* **33**, 12746–12751.

Siegel, R.W., Jain, R. & Bradbury, A. (2001) Using an *in vivo* phagemid system to identify non-compatible *lox*P sequences. *FEBS Lett.* **505**, 467–473.

Thyagarajan, B., Olivares, E.C., Hollis, R.P., Ginsburg, D.S. & Calos, M.P. (2001) Site-specific genomic integration in mammalian cells mediated by phage phiC31 integrase. *Mol. Cell. Biol.* **21**, 3926–3934.

Wirth, D., Gama-Norton, L., Riemer, P., Sandhu, U., Schucht, R. & Hauser, H. (2007) Road to precision: recombinase-based targeting technologies for genome engineering. *Curr. Opin. Biotechnol.* **18**, 411–419.

Received: 7 January 2011
Accepted: 29 March 2011

Supporting Information/Supplementary material

The following Supporting Information can be found in the online version of the article:

Figure S1 Recombination efficiencies of RMCE products using wtFLP. The bands of P6.0 in Fig. C1, lanes 7–12, are shown together with those of the Substrate in the negative control in Fig. C1, lane 13, are shown. The result of one dose-dependent experiment was shown for wtFLP and was very similar to that for FLPe shown in Fig. C2.

Additional Supporting Information may be found in the online version of this article.

Please note: Wiley-Blackwell are not responsible for the content or functionality of any supporting materials supplied by the authors. Any queries (other than the missing material) should be directed to the corresponding author for the article.

Published online 4 November 2010

Nucleic Acids Research, 2011, Vol. 39, No. 2 e7
doi:10.1093/nar/gkq966

High-level expression by tissue/cancer-specific promoter with strict specificity using a single-adenoviral vector

Yumi Kanegae*, Miho Terashima, Saki Kondo, Hiromitsu Fukuda, Aya Maekawa, Zheng Pei and Izumu Saito

Laboratory of Molecular Genetics, Institute of Medical Science, University of Tokyo, 4-6-1 Shirokanedai, Minato-ku, Tokyo 108-8639, Japan

Received March 26, 2010; Revised September 24, 2010; Accepted October 3, 2010

ABSTRACT

Tissue-/cancer-specific promoters for use in adenovirus vectors (AdVs) are valuable for elucidating specific gene functions and for use in gene therapy. However, low activity, non-specific expression and size limitations in the vector are always problems. Here, we developed a 'double-unit' AdV containing the Cre gene under the control of an α-fetoprotein promoter near the right end of its genome and bearing a compact 'excisional-expression' unit consisting of a target cDNA 'upstream' of a potent promoter between two *lox*Ps near the left end of its genome. When Cre was expressed, the expression unit was excised as a circular molecule and strongly expressed. Undesired leak expression of Cre during virus preparation was completely suppressed by a dominant-negative Cre and a short-hairpin RNA against Cre. Using this novel construct, a very strict specificity was maintained while achieving a 40- to 90-fold higher expression level, compared with that attainable using a direct specific promoter. Therefore, the 'double-unit' AdV enabled us to produce a tissue-/cancer-specific promoter in an AdV with a high expression level and strict specificity.

INTRODUCTION

Because tissue-specific promoters enable us to express a gene in a cell-type-specific manner *in vivo* or in a primary tissue culture, such promoters offer an attractive approach to studying the specific functions of a gene product in the tissues of experimental animals, such as in the brain where cells of different types are present together in the same region. The use of transgenic/knockout mice and adenovirus vectors (AdVs) are the most common approaches for utilizing these promoters. Among such promoters, those specific to malignant cells may be valuable for specific gene therapy or the diagnosis of cancer.

However, one drawback of such promoters is that their expression levels are much lower than those of a versatile promoter, such as the cytomegalovirus (CMV) immediate-early, CAG (1) or EF1α (2) promoters. For example, the α-fetoprotein (AFP) promoter, which is a relatively strong promoter among tissue-specific promoters, is reported to be ~500-fold less active than the CAG promoter (3), limiting its usefulness. Another important problem associated with the use of these promoters is that their specificity was often not sufficiently strict. One possible reason is that the excised segment of a specific promoter lacks the sufficient control of specific silencers and shows some 'basal level' of expression. In some cases, the lack of specificity might arise from the DNA elements surrounding the promoter, rather than the intrinsic character of the specific promoter (4,5). In human gene therapy using AdV, a strict specificity is critically important for safety as well as efficacy.

As one solution, we previously reported a 'double-infection' method (3), in which the virtual activity of AFP promoter was increased by about 50-fold while maintaining a strict specificity. With this method, two AdVs are infected simultaneously: one AdV contains a 'switch unit' consisting of Cre gene under the control of AFP promoter, and the other AdV bears a 'target unit' consisting of the CAG promoter,

*To whom correspondence should be addressed. Tel: +81 3 54495556; Fax: +81 3 5449 5432; Email: kanegae@ims.u-tokyo.ac.jp
Present addresses:
Saki Kondo, Cell Regulation Laboratory, Paterson Institute for Cancer Research, University of Manchester, Wilmslow Road, Manchester, M20 4BX, UK
Hiromitsu Fukuda, Japan Animal Referral Medical Center, 2-5-8 Kuji, Takatsu-ku, Kawasaki-shi, Kanawawa 213-0032, Japan

*lox*P, the stuffer sequence, second *lox*P, and a target cDNA, in that order. In non-hepatocarcinoma cells, the expression of the reporter cDNA remains turned off. However, in target hepatocarcinoma cells, AFP promoter in the switch unit of one AdV is turned on, leading to the production of Cre enzyme; this in turn leads to the excision of the stuffer sequence in the other AdV by Cre-mediated site-specific recombination, leaving the CAG promoter and the target gene connected only through a *lox*P sequence and enabling the strong expression of the target gene. Even when AFP promoter is weak and only a small quantity of Cre protein is produced, Cre can act as an enzyme multiple times, allowing most of the target AdV genomes to be processed eventually and accounting for the very high level of expression that can be obtained. The double infection method has been applied in numerous *in vivo* studies examining gene therapy for lung, colon and gastric cancers using the carcinoembryonic antigen promoter (6–10), for thyroid cancer using the thyroglobulin promoter (11), for hepatocellular carcinoma using AFP promoter (12), for prostate cancer using the prostate-specific antigen promoter (13) and for astrocytoma using the astrocytoma-specific promoter for GFAP (14). The method has also been applied in brain research using a modified, neuron-specific promoter of superior cervical ganglion 10 (15).

However, because the double-infection method uses two different AdVs simultaneously, controlling the infection is complicated and not often reproducible. Additionally, the toxicity and inflammation are at least doubled, compared with a single viral infection, for transducing the same amount of the target unit. Moreover, since a single cell infected with only one of the vectors does not produce any target protein, many such cells remain unused, causing a low expression as a result of dilution (12). Therefore, as a simpler, safer and more effective vector, an AdV bearing both the switch and the target unit simultaneously in a single genome is needed. However, the development of such an AdV has been regarded as being very difficult, since the sum of the lengths of both units exceeds the maximum length of the AdV genome. Furthermore, a leak in the expression of Cre can produce a large amount of stuffer-lacking AdV during vector preparation, causing severe non-specific expression. In addition, an enhancer of the potent promoter in the target unit may decrease the specificity of the specific promoter in the switch unit. Thus, a new vector is needed to solve these problems.

Here, we report the development and successful preparation of an AdV containing both units in a single genome. The vector, called a 'double-unit' AdV, possesses an extraordinary 'excisional-expression' structure and solves the aforementioned problems simultaneously, because the target unit of this vector lacks a stuffer sequence and because the target gene is expressed not from its genome, but from an excised circular DNA. The developed AdV shows a high level of expression (40- to 90-fold) while maintaining a very strict specificity.

MATERIALS AND METHODS

Cells and AdVs

The human embryo kidney cell line, 293 (16), constitutively expresses adenoviral E1 genes and supports the replication of E1-substituted AdV. HepG2 (17) and HuH7 (18) cells are human hepatocellular carcinoma cell lines that produce AFP. SK-Hep-1 (19) cells are a human hepatocellular carcinoma cell line that lack AFP production. HeLa cells, derived from cervical cancer, do not express AFP (20). The cell line CV1 is derived from African green monkey kidney. The AFP promoter used here was the (AB)2S6 AFP promoter (3). The EF1α promoter has been described previously (2). AxA2ANCre was described previously (3). AxLR14EL-AC, AxLR16EL-AC, AxLR16EFL, Ax-AC, AxNZ, AxLNZCAL, AxALNZCAL, AxA2AdsR and AxEFdsR are described for the first time in this work. AdVs described here were constructed using cosmid transfection (21). All the aforementioned viruses except for AxA2AdsR and AxEFdsR possessed E3 region with a 2.4-kb deletion, while the latter two viruses bore E3 region with the 1.9-kb deletion described in reference (21) (see 'Discussion' section). The switch unit was inserted at the *Sna*BI site (nt position 35 770), located 165-nt downstream from the right end of the adenovirus-5 (Ad5) genome. Because the standard Ad5 genome does not contain the *Sna*BI site, we generated a restriction site using nucleotide substitution, inserted a *Swa*I linker, and then cloned the switch unit. All the viruses were purified using a CsCl step gradient (22) and titrated using a method measuring 50% tissue culture infectious dose ($TCID_{50}$) (22); the viral particle: $TCID_{50}$ ratio was ~20:100, including double-unit viruses. The viral titer of all the AdV, including double-unit vectors was measured with $TCID_{50}$ using normal 293 cells.

Dominant negatives and shRNAs of Cre and isolation of Cre-suppressed 293 cells

dnCreRY was a dominant negative of Cre, where Arg173 and Tyr324 were mutated to Ala and Phe, respectively. pyCANCRYit2 is a plasmid expressing dnCreRY under the control of CAG promoter. The dnCreRY cDNA was excised as a *Sma*I-*Bgl*II fragment and inserted into pTrcHis2A (Invitrogen) between the *Ecl*36II and *Bgl*II sites under the *Escherichia coli* trc promoter (23). The *Bss*SI-*Sph*I fragment containing trc-dnCreRY was transferred upstream of the cos site of cosmid pAxLR16EL-AC and pAxLR14EL-AC, which were both derived from pAxcwit2 (21). The resulting cosmids were named ptdC-AxLR16EL-AC and ptdC-AxLR14EL-AC, respectively. shCreD (TA0493-4-D) was an shRNA of Cre, gatccGAAGCAACTCATCGATTGAtagtgctcctg gttgTCAATCGATGAGTTGCTTCtttttta (Cre sequences are in capitals), which efficiently suppressed Cre activity. TA0493-4-D was inserted under the human U6 promoter of plasmid pBAsi hU6 Pur (Takara Bio). The 293dnCreRY8 and 293shCreD13 were the best cell lines containing dnCreRY under the control of CAG promoter

and shCreD driven by human U6 promoter suppressing Cre activity among those tested, respectively.

To generate 293dnCreRY8, pBCANCRYSAPur was constructed, expressing dnCreRY under the control of the CAG promoter and the puromycin-resistant (Pur^R) gene under the control of the SV40 early promoter (Figure 5a). To generate 293shCreD13, pBSAPurhU6shCre was constructed, expressing one of the short-hairpin (sh) RNAs against Cre under the control of the human U6 promoter (Takara Bio) and the Pur^R gene identical to that expressed by pBCANCRYSAPur (Figure 5b). Ten micrograms of each plasmid DNA were transfected into 293 cells using Transfast^R (Promega). Two days after transfection, puromycin was added at a concentration of 2.5 μg/ml. We selected the cell line that most efficiently caused a reduction of Cre activity for the simultaneous transfection in Cre-expressing and target pCALNLG plasmids (24).

Preparation of total cell DNA for restriction-enzyme digestion and for real-time PCR

Infected cell DNA was prepared on a 24-well plate as previously described (25) with some modifications: the cells were suspended in 0.4 ml of TNE-PK [50 mM Tris–HCl (pH 8), 100mM NaCl, 10 mM EDTA, 100 mg/ml proteinase K], followed by the addition of SDS (final 0.1%). After incubation at 55°C for 2 h, the mixture was extracted once with phenol–chloroform and once with chloroform, and precipitated with 1 or 1.5 volumes of ethanol at −20°C for >1 h and then washed once with 70% ethanol. The pellet was dissolved with 50 ml of TE containing 20 mg/ml RNase A and stored at −20°C. This DNA was sufficient not only for real-time PCR but also for gel electrophoresis to observe the structure of the AdV genome.

To detect viral DNA, total DNA extracted from AxLR16EL-AC-infected, Cre-suppressed 293 cells in a 24-well plate was digested with *Bmg*BI. The *Bmg*BI recognition sequence, CACGTG, contains a -CG- dinucleotide, which is mostly methylated in the mammalian genome and cannot be cleaved by a restriction enzyme, while replicating adenoviral DNA is not methylated and can be cleaved. Consequently, restricted patterns of only adenoviral DNA can be seen.

Quantification of AdV transduction efficiency and expressed RNA

Total cell DNA was prepared as described above. Real-time PCR was performed to detect the adenovirus genome using a probe for the pIX gene, and human chromosome was simultaneously detected using a probe for the β-actin gene or the ornithine transcarbamylase (OTC) gene. The threshold cycle (cT) values were obtained. All the probes used in the study are shown in Table 1. The cT value of the AdV was corrected according to that for the human chromosome probe. The sequences of these probes were shown in Table 1. Infected cell RNA was prepared using the RNeasy protect mini kit (Qiagen) according to the manufacturer's protocol. To prepare the cDNA, the TaqMan Reverse Transcriptase Reagent kit (Applied BioSystems) was used. The sequences of the dsRed probes are shown in Table 1. The 18S rRNA primer used in the study were Ribosomal Eukaryotic 18S rRNA kit (Applied BioSystems).

Table 1. Sequences of probes used in real-time PCR

Probe[a]	Primer sequences[b]
AdV-1	F: TGTGATGGGCTCCAGCATT
	P: ATGGTCGCCCCGTCCTGCC
	R: TCGTAGGTCAAGGTAGTAGAGTTTGC
hOTC-1	F: CCACTACAAAATAAAGTGCAGCTGAA
	P: CCGTGACCTTCTCACTCTAAAAAACTT
	R: CTGATAGCCATAGCATATATTTAATTTCTTCTC
β-Act-1	F: CTCGCAGCTCACCATGGAT
	P: ATGATATCGCCGCGCTCGTCGT
	R: ATGCCGGAGCCGTTGTC
dsRed-1	F: GCAGCTGCCCGGCTACT
	P: CGTGGACTCCAAGCTGGACATCACCT
	R: CGATGGTGTAGTCCTCGTTGTG

18S rRNA primers used were Ribosomal Enkaryotic 18S rRNA kit (Applied BioSystems).
[a]Name of the probes. Reporters used were FAM except β-Act-1 (VIC reporter).
[b]F, forward primer; P, probe; R, reverse primer. Real-time PCR was purchased from Applied BioSystems.

To examine the expressed dsRed RNA, the cells were infected with AdV and total DNA and the total RNA was extracted. From the total DNA, the amounts of AdV genome and β-actin gene were simultaneously quantified using real-time PCR and the ratio of AdV genome per cell was obtained. Similarly, from the total RNA, the amounts of dsRed RNA and 18S-rRNA (the correction standard) were quantified using reverse transcription and real-time PCR, and the ratio of dsRed RNA to 18S-rRNA was obtained. Based on these results, the ratio of the dsRed RNA level between the two cell lines was calculated.

Detection of expressed fluorescence

To evaluate the different EF1α promoter versions, the cells were washed twice with Hank's balanced salt solution 3 days after transfection, and the intensity of GFP fluorescence was quantified using Fluoroskan Ascent FL (Labsystems) (26). Cells infected with AxLR16EL-AC and AxLR14EL-AC were sorted using dsRed fluorescence using FACS (FACSCalibur, Becton-Dikinson). The dsRed fluorescence was also measured using Ascent fluorescent meter. To calculate the relative strengths among the various promoters, the steady-state level of the expressed dsRed RNA together with the dsRed DNA in the AdV genome in infected cells was quantified using a real-time PCR (Prism 7000, Applied Biosystems), and the former value was divided by the latter.

RESULTS

Structure of 'double-unit' vector containing 'excisional-expression' unit

The structure of the 'double-unit' AdV vector AxLR16EL-AC is shown in Figure 1. This vector is a